JOURNAL OF GEOPHYSICAL RESEARCH: ATMOSPHERES, VOL. 118, 1–14, doi:10.1002/jgrd.50442, 2013

Three years of lightning impulse charge moment change measurements in the United States

Steven A. Cummer,[1] Walter A. Lyons,[2] and Mark A. Stanley[3]

Received 21 August 2012; revised 16 April 2013; accepted 23 April 2013.

[1] We report and analyze 3 years of lightning impulse charge moment change (iCMC) measurements obtained from an automated, real time lightning charge moment change network (CMCN). The CMCN combines U.S. National Lightning Detection Network (NLDN) lightning event geolocations with extremely low frequency ($\lesssim$ 1 kHz) data from two stations to provide iCMC measurements across the entire United States. Almost 14 million lightning events were measured in the 3 year period. We present the statistical distributions of iCMC versus polarity and NLDN-measured peak current, including corrections for the detection efficiency of the CMCN versus peak current. We find a broad distribution of iCMC for a given peak current, implying that these parameters are at best only weakly correlated. Curiously, the mean iCMC does not monotonically increase with peak current, and in fact, drops for positive CG strokes above +150 kA. For all positive strokes, there is a boundary near 20 C km that separates seemingly distinct populations of high and low iCMC strokes. We also explore the geographic distribution of high iCMC lightning strokes. High iCMC positive strokes occur predominantly in the northern midwest portion of the U.S., with a secondary peak over the gulf stream region just off the U.S. east coast. High iCMC negative strokes are also clustered in the midwest, although somewhat south of most of the high iCMC positive strokes. This is a region far from the locations of maximum occurrence of high peak current negative strokes. Based on assumed iCMC thresholds for sprite production, we estimate that approximately 35,000 positive polarity and 350 negative polarity sprites occur per year over the U.S. land and near-coastal areas. Among other applications, this network is useful for the nowcasting of sprite-producing storms and storm regions.

Citation: Cummer, S. A., W. A. Lyons, and M. A. Stanley (2013), Three years of lightning impulse charge moment change measurements in the United States, *J. Geophys. Res. Atmos*, *118* , doi:10.1002/jgrd.50442.

1. Introduction

[2] Automated and geographically extensive remote measurements of lightning parameters are a valuable class of tool in lightning research. The most widely estimated parameter, aside from location and polarity, is return stroke peak current, which can be remotely estimated from the low frequency radiation [*Willett et al.*, 1988; *Cummins et al.*, 1998a] from lightning. This radiation can be measured hundreds of kilometers from the lightning stroke. The significance of lightning peak current is driven by its connection to phenomena such as power line flashover [*Cummins et al.*, 1998b; *Rakov and Uman*, 2003, p. 616] and electromagnetic pulse effects in the ionosphere [*Taranenko et al.*, 1993].

[3] Another parameter that can be measured from electromagnetic fields long distances from the lightning stroke is charge moment change (CMC), which is the product of charge transfer and the vertical distance over which that charge is transferred (and thus the units are coulomb-kilometers or C km). CMC can be remotely estimated from extremely low frequency (ELF, 3–3000 Hz) radiation [*Jones and Kemp*, 1971; *Burke and Jones*, 1996; *Huang et al.*, 1999; *Cummer and Inan*, 2000; *Hobara et al.*, 2001], and has proven important for understanding the origins of lightning-driven high-altitude electric breakdown in the form of sprites [*Pasko et al.*, 1997], is linked to heating and damage at a lightning contact point [*Rakov and Uman*, 2003, p. 589], and may also be connected to forest fire ignition [*Fuquay et al.*, 1972; *Latham and Schlieter*, 1989].

[4] Charge and transfer length are not separable in ELF measurements if the vertical channel length (roughly 5–10 km for lightning) is significantly shorter than an electromagnetic wavelength (300 km at 1 kHz) because of the electromagnetic fields created by an electrically small linear antenna [*Inan and Inan*, 2000, p. 652]. Thus 10 C removed

[1]Electrical and Computer Engineering Department, Duke University, Durham, North Carolina, USA.
[2]FMA Research, Fort Collins, Colorado, USA.
[3]Langmuir Laboratory, Geophysical Research Center, New Mexico Tech, Socorro, New Mexico, USA.

Corresponding author: S. A. Cummer, Electrical and Computer Engineering Department, Box 90291, Duke University, Durham, NC 27708, USA. (cummer@ee.duke.edu)

2169-897X/13/10.1002/jgrd.50442

from 10 km and 20 C removed from 5 km are both a 100 C km charge moment change and produce the same distant signal at ELF frequencies. Additionally, distant ELF measurements are only sensitive to vertical channel length, because horizontal channel components produce an oppositely directed image current in the ground and thus do not radiate significantly [*Wait*, 1970, p. 173].

[5] Global measurements of lightning CMC over months to years have been performed using Schumann resonance-band ($\lesssim$ 50 Hz) electromagnetic measurements [*Füllekrug and Constable*, 2000; *Sato and Fukunishi*, 2003; *Yamashita et al.*, 2009]. Because of typically high background noise, these measurements are only sensitive to the very highest charge transfer lightning strokes, however, and are thus distinct from those reported here, which include both strong and modest lightning strokes. The higher frequency ELF signals used here have been used to measure CMC in specific events of interest [*Cummer and Inan*, 1997] and in many lightning strokes from an individual storm [*Cummer and Lyons*, 2004], but to our knowledge have not been previously applied to millions of lightning events, yearly time scales, and continental spatial scales.

[6] Here we report and analyze 3 years of measurements from an automated, real time lightning Charge Moment Change network (CMCN). The CMCN contains only two sensor stations, but because of the long reach of ELF measurements, lightning in most of the U.S. is measured. By design the CMCN uses lightning geolocations from the U.S. National Lightning Detection Network (NLDN) operated by Vaisala, Inc. We use herein the following terminology: a detected and processed lightning signal is termed a lightning event, an NLDN-classified event is an NLDN report, and each NLDN report is classified as either a cloud pulse (also sometimes an in-cloud (IC) event) or a cloud-to-ground stroke (CG). We specifically avoid using the term IC stroke.

[7] The parameter measured by the CMCN is impulse charge moment change (iCMC), defined as the total charge moment change over the first 2 ms of the lightning stroke. This parameter effectively measures the charge moment change of the return stroke [*Rakov and Uman*, 2003, p. 176] and perhaps some short continuing current (although where the precise boundary is between return stroke and continuing current is difficult to say). Although longer duration charge transfer that occurs in long continuing current can be measured at long ranges with magnetic field measurements [*Williams and Brook*, 1963; *Cummer and Füllekrug*, 2001; *Ross et al.*, 2008], doing so reliably requires very low noise measurements and careful processing that are challenging to implement in a real-time system.

[8] Our primary goal is to report the basic statistics of lightning iCMC over a large spatial region (the contiguous U.S.) and a long time window (36 months). Section 2 describes the sensors, system architecture, and processing, and section 3 presents a brief summary of the 36 months of data and validation. The analyzed lightning iCMC distributions are reported in sections 4.1 and 4.2, and their implications for sprite occurrence rates are discussed in section 4.3. The relationship between NLDN-reported peak current (I_{pk}) and iCMC is examined in detail in section 4.4, and one main finding is that although these parameters are connected, there is a wide distribution of iCMC for a given I_{pk}. This indicates that these parameters are to some degree independent, which has been found in more precise measurements of much smaller lightning populations [*Berger et al.*, 1975; *Schoene et al.*, 2010] and is likely at least partly due to different flash morphologies producing significantly different iCMCs even for similar values of I_{pk} [*Lu et al.*, 2012]. For many values of I_{pk}, especially for positive polarity events, the iCMC distribution is bimodal. One possible cause is that the two peaks represent in-cloud (IC) pulses and cloud-to-ground (CG) strokes. If so, the iCMC may provide valuable information on distinguishing these types of strokes, but further research is needed to determine the origin of these distinct iCMC populations. Section 5 explores in detail the geographic distributions of different classes of high iCMC events.

2. Description of the CMCN

[9] For the period studied, the CMCN was composed of two sensor stations. One operated near Duke University in North Carolina at 35.975°N latitude and –79.100°E longitude, and the other at Yucca Ridge near Fort Collins, Colorado at 40.668°N latitude and –104.937°E longitude. Figure 1 shows a map of these two sites and, for reference, the 1000 and 2000 km radius circles centered about these sites. These two sites have proven sufficient to provide meaningful measurements over most of the continental United States, with some limitations discussed below in section 2.3.

2.1. Sensors and Data Acquisition

[10] Each site contains two orthogonal induction magnetic field sensors (built by Quasar Federal Systems, Inc.) with a gain of 0.3 V/nT that measures the horizontal vector magnetic field from lightning discharges. These sensors have a flat response from about 2 Hz to 25 kHz and thus measure the very low frequency (VLF, 3–30 kHz) and ELF emissions. The signals are filtered with a 6 pole, 25 kHz low pass filter and sampled at 100 kHz. The sensors were calibrated by the maker of the coils, and this calibration was verified by comparing signals measured in the field with those from independently calibrated sensors at the same site.

[11] The signals processed by the CMCN are recorded with a triggered data acquisition system with GPS timing for high absolute time accuracy. The trigger window is 10 ms, with 2.5 ms of pre-trigger recording and 7.5 ms post-trigger. The system has a trigger criterion based on signal amplitude after real-time processing to estimate and subtract the power line noise. This trigger is thus based on peak value of the time domain VLF waveform, which is statistically correlated with the NLDN-measured peak current of the source stroke [*Lu et al.*, 2011], and also depends on propagation distance. Smaller peak current and longer propagation distance lightning strokes are less likely to trigger the system and thus be measured by the CMCN. The two systems have different trigger thresholds (2.0 nT at Duke and 3.3 nT at YRFS, not time varying) that reflect the different noise and background thunderstorm environments, and this does influence the distribution of lightning strokes measured by each system (see sections 3.1 and 4.1). However, highly energetic lightning strokes are the primary focus of this analysis, and these generally have a high enough amplitude to trigger the sensors regardless of distance or the system details.

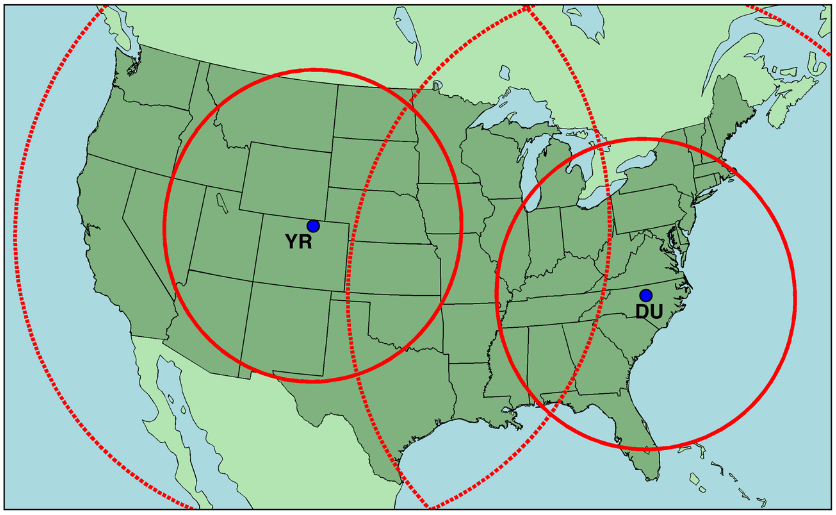

Figure 1. Map showing the location of the two sensors (DU and YR), and for reference 1000 km (solid red) and 2000 km (dashed red) radius circles around each location.

2.2. Data Processing

[12] This system is designed to operate in near real time to show which storms are producing high charge transfer lightning. The triggered waveforms are thus recorded at each site in 5 min blocks. After each data block is recorded, the data files are transferred via a network connection to a central processing computer. As we do not perform lightning geolocation, we depend on real time millisecond-timing stroke-level NLDN data [*Cummins and Murphy*, 2009] provided by Vaisala, Inc. The processing first involves checking every CMCN trigger for timing consistency with any possible NLDN-reported discharge to identify the location of as many CMCN triggers as possible. When a match is found, it is usually unambiguous (some limitations are discussed in the section below) and yields the location for a significant fraction of the CMCN triggers. This matching thus provides the stroke-to-sensor propagation distance that is needed for quantitative processing of the signals.

[13] CMCN triggers associated with an NLDN event of peak current less than 10 kA in magnitude are not processed, because there are frequently too many of these to be easily processed in real time. For every CMCN trigger with a corresponding NLDN lightning location and peak current above 10 kA magnitude, the system computes the azimuthal magnetic field waveform by appropriately rotating the two orthogonal signals and filters the data to yield a <1 kHz signal for each stroke to be processed. This signal and the known propagation distance are used to compute the vertical impulse charge moment change (iCMC) using a version of the regularization-based technique described in detail by *Cummer and Inan* [2000]. This analysis must be fast enough that all of the triggers in a 5 min block can be processed in less than 5 min to be ready for the next block. Minimal consistency checking to identify and limit the impact of noise is applied, and for a single lightning stroke, the realtime iCMC will not be as reliable as one computed with more careful and time-consuming processing. See section 3.1 for more details of the statistical properties of these measurements. Section 2.3 discusses additional post-processing to remove several classes of known erroneous event measurements.

[14] This approach uses an Earth-ionosphere waveguide simulation to compute the < 1 kHz propagation impulse response, which automatically includes both radiation and induction magnetic fields and also the critical waveguide effects. One of three different electron density profiles corresponding to midday, morning/evening, and nighttime conditions, is used for the computation depending on the local time of the midpoint of the propagation path.

[15] The data streams from the two sensor locations are processed independently, which means that big discharges may trigger both systems and thus provide two independent measurements of the same lightning. In section 3.1, we examine this subset of the data to show that the independent measurements are generally in good agreement. In the overall data set, when two measurements are available, the Duke measurement is taken as the official value because of lower background noise at the sensor site.

[16] The end result is a set of iCMC measurements for many NLDN-detected strokes delivered in near real time. The total latency is between 7 and 12 min from the lightning stroke from the 5 min acquisition file duration, file transfer time, and processing time. Figure 2 shows an example of a near real time plot that can be generated from this system, displaying the high iCMC lightning strokes coded by polarity and occurrence time. Plots like these have proven extremely useful in determining where to point a camera targeting high altitude transient luminous events (TLEs) [*Lyons et al.*, 2009; *Lang et al.*, 2010]. Anecdotally, we have periodically observed sprites from storms that appear from radar and infrared satellite images to be too small to generate sufficiently energetic lightning and thus would not normally have been targeted, but that the CMCN says (correctly) were producing high iCMC lightning.

2.3. Network Limitations and Post Processing

[17] As in any operational system, the CMCN has certain limitations that can influence the measurements. We attempt to identify the most significant ones here and discuss the post-processing that eliminates known errors. As noted above, lightning strokes with NLDN peak current

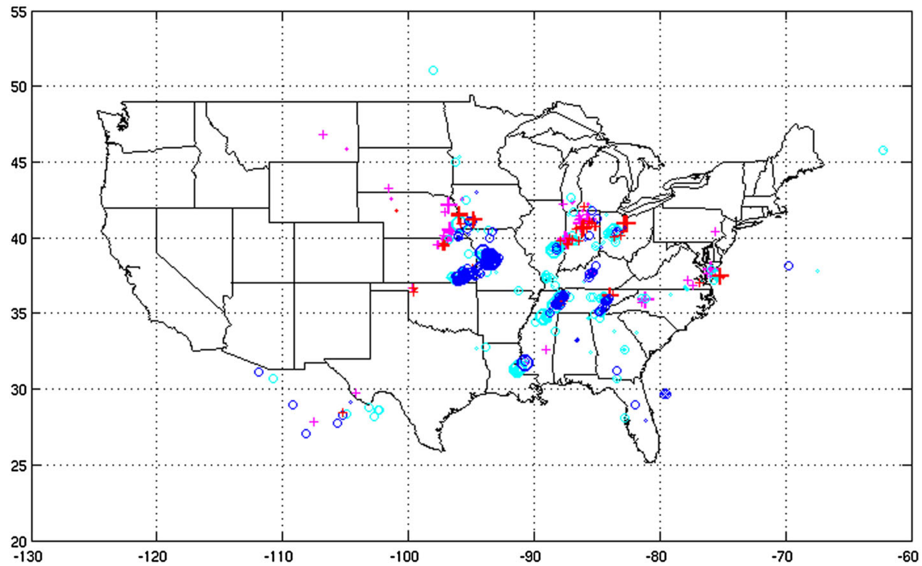

Figure 2. Example of a real time iCMC map delivered by the CMCN, showing high iCMC strokes over a 3 h period ending on 20 August 2009, 02:20 UT. The red crosses are locations of high iCMC positive lightning, and the blue circles are locations of high iCMC negative lightning. The size of the symbol denotes the iCMC magnitude.

magnitudes less than 10 kA are intentionally not processed, and this obviously influences the distributions presented below, particularly for in-cloud (IC) lightning. Because we rely on the NLDN for lightning detection, signals from any lightning stroke not reported by the NLDN are not processed. Although the majority of lightning strokes are NLDN-reported [*Cummins and Murphy*, 2009], even high peak current strokes are occasionally missed and thus not measured by the CMCN, due to challenges in processing the very complex signals. The NLDN data also infrequently contain known artifacts, such as nonphysical doublets (two reported NLDN strokes for what is likely a single event), and these are removed in post-processing.

[18] Occasionally, a small signal from a local thunderstorm will trigger the acquisition system at a time that is consistent with a more distant NLDN-reported stroke and thus yield an incorrect stroke location identification. This leads to a completely erroneous iCMC measurement. These events can usually be identified because the distant stroke peak current is clearly too small to have triggered the system, and almost all of these are removed in real time processing and post-processing.

[19] The CMCN exhibits some degree of blindness to some high iCMC events at ranges closer than several hundred km. These lightning events trigger the system and are thus processed, but the signal is saturated and thus amplitude limited. This results in a measured iCMC that is much smaller than it actually is. This issue is also discussed below in sections 5.1 and 5.2. The system relies on the NLDN-reported lightning polarity, and if this is incorrect (as it sometimes is especially for complex strokes), then the reported iCMC is wrong and almost certainly too small.

[20] Lastly, the triggering criterion means that lower peak current and more distant lightning strokes are less likely to trigger the system. This means that the measurements exclude many modest I_{pk} return strokes that are not close to either sensor. However, the statistical distribution of I_{pk} for all CMCN measured strokes (see section 4.1) contains millions of strokes at small I_{pk} values, and thus events over the full range of lightning strength are robustly measured by the CMCN. We also correct for this I_{pk}-dependent triggering as described in section 4.1.

3. CMCN Data Summary

[21] The CMCN system has run nearly continuously since June 2007. From August 2007 to July 2010 (36 months), there were a total of 33 days missing data from the DU sensors, and 24 days missing data from the YR sensors (thus an uptime of about 97%). It is this 3 year window that we have analyzed and for which we present fundamental statistics in the following sections. The data have been post-processed to remove known problems as discussed in section 2.3, which reduced the data volume by a bit less than 1%.

[22] After this post-processing, a total of 13,570,866 lightning events were measured over these 36 months. NLDN reported that approximately 12.1 million were negative polarity, 1.4 million were positive polarity, 13.1 million were cloud-to-ground (CG), and 455,000 were in-cloud (IC). Recall that the processing threshold of 10 kA filters out the majority of IC events. For reference, during the same 36 month period, NLDN reported 172 million total strokes above 10 kA peak current, and 147 million of those were classified as CG.

3.1. Measurement Consistency

[23] Validating these measurements is a challenge. Lightning charge moment change measurements using remote magnetic field measurements and our basic approach, albeit with more complex processing, have been validated previously [*Ross et al.*, 2008] by separately analyzing electric and magnetic field measurements. We have anecdotally compared measurements from the CMCN system to those obtained with more complex processing of data

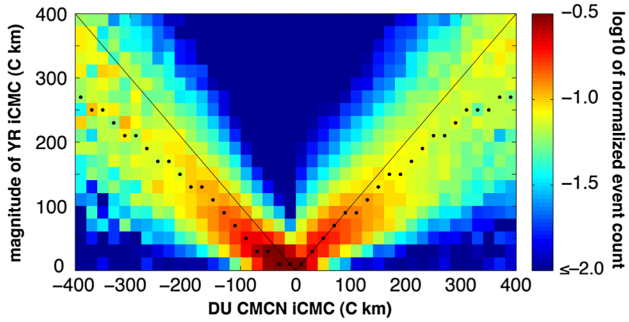

Figure 3. Normalized scatter density plot of the iCMC measured by the YR and DU systems for the same event. The unit slope lines denote the ideal, and the dots mark the median YR value for each DU bin. The close statistical agreement between the two independent measurements confirms their validity.

from the magnetic field coils used in previous studies [*Cummer and Inan*, 2000; *Li and Cummer*, 2012] and found good agreement.

[24] The CMCN data themselves provide one avenue for confirming the consistency of the data. The amplitude-dependent trigger threshold means that the large majority of discharges are measured by only one of the two CMCN stations. However, high I_{pk} strokes sometimes trigger both systems and two independent iCMC values are measured. Over the three years analyzed here, there were almost 393,000 strokes (about 2.8% of the total) that were measured by both systems. Ideally these measurements would be identical, and the differences analyzed below provide some insight into the consistency of the automated measurements.

[25] Figure 3 shows a normalized scatter density plot of the iCMC values reported by each system (DU and YR) for these 393,000 strokes. Negative strokes are on the left and positive on the right. The iCMC values are binned with 20 C km resolution and then normalized so that each vertical slice on the plots represents the probability distribution function of the YR iCMC for a given DU iCMC. Also plotted are the median YR iCMC values for each DU iCMC bin and the unit slope lines for reference.

[26] There is an apparent bias towards smaller iCMC values from the YR sensors, and this is consistent for both positive and negative strokes. A quantitative comparison of the two values for all events above 20 C km reveals that the mean of the ratio of the YR and DU measurements is 0.79. We are currently investigating the source of this bias and hope to correct it in the future. No correction is made to the data herein to account for the bias, but such a correction would not affect the main conclusions of the work.

[27] For individual events, we find that the ratio of the larger to the smaller of the two reported iCMC values is less than 1.6 for more than 50% of the events. This difference reflects the independent noise environments, both natural and anthropogenic, at each measurement site. When limited to strokes with iCMC > 100 C km, this measurement discrepancy drops further, indicating that measurement noise (especially for smaller strokes) is responsible for a significant fraction of the discrepancy in individual events. Consequently, automated measurements for a single stroke from our CMCN system should be considered accurate to within a factor of about 1.5. The distribution of the differences (Figure 3) shows that this uncertainty does not affect the statistical results presented here, and importantly, this means when a high iCMC stroke occurs, both stations almost always agree that it is a high iCMC stroke. Higher precision and reliability can be obtained with more consistency checks built into the data processing, but it is challenging to implement more complex algorithms in real time.

4. Statistical Distributions of the iCMC Data Set

[28] We now present a detailed analysis of the 13.6 million events whose iCMC was measured by the CMCN, including a correction for the limited detection efficiency of smaller I_{pk} lightning. We focus primarily on the statistical distributions of iCMC as a function of lightning polarity, independent of geographic location. This enables us to determine how frequent, in an absolute and relative sense, are lightning strokes of a given iCMC. We also discuss the implications of these occurrence rates for the production of sprites.

4.1. Detection Efficiency and NLDN Peak Current Distributions

[29] We first examine the detection performance of the CMCN. Figure 4(top) shows the computed detection efficiency (DE) of the CMCN system as a function of NLDN peak current. DE is defined as the ratio of detected and processed lightning events to the total number of NLDN-detected events. Recall that the CMCN has a trigger

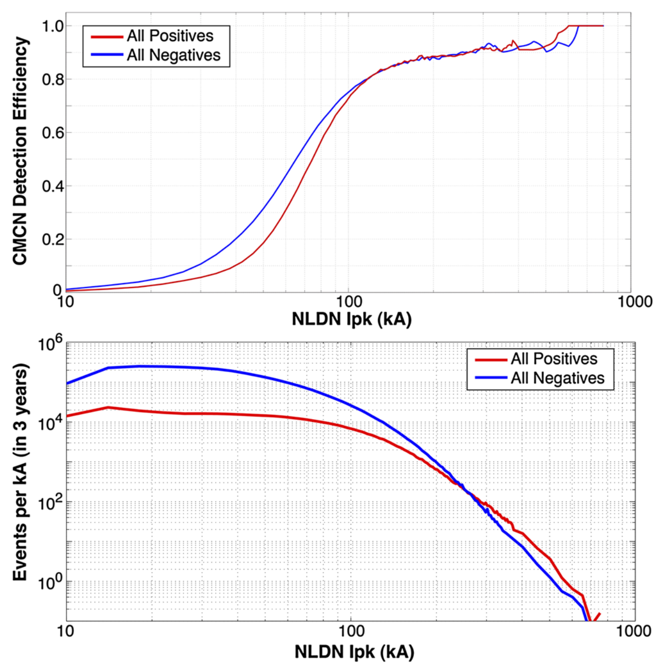

Figure 4. (top) Detection efficiency (DE) of the CMCN versus NLDN I_{pk}. DE drops with peak current because of the amplitude-dependent triggering of the CMCN. (bottom) Distributions of NLDN-reported peak current for all CMCN-processed lightning events in the 3 year analysis window. Despite the low DE at low NLDN I_{pk}, the CMCN-measured events span the entire range of peak current and still include millions of low I_{pk} events.

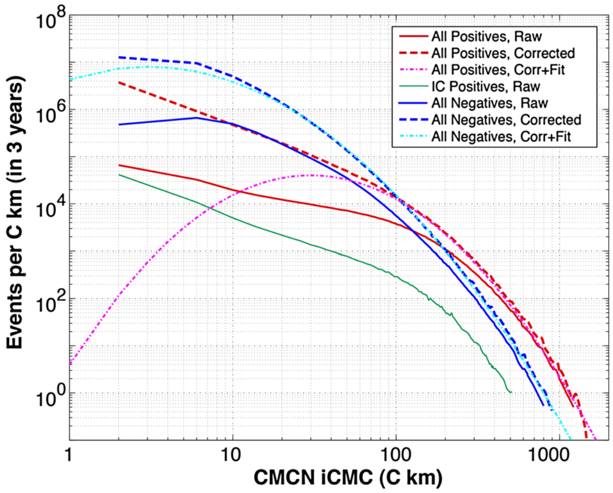

Figure 5. (solid lines) Raw, directly measured distributions of iCMC for all CMCN-processed lightning events in the 3 year analysis window. Plotted separately are the measured distributions for all positive, all negative, and all positive IC events. (dashed lines) Corrected distributions of iCMC for all positive and all negative events that compensate for the reduced detection efficiency for lower I_{pk} events. (dash-dot lines) Log-normal fits to the corrected positive and negative distributions.

threshold that is correlated with peak current and inversely with propagation distance. Thus, smaller discharges more distant from the two sensors are less likely to be measured by the system. The resulting detection efficiency is 75% and higher for lightning events above 100 kA and much lower for weaker events, falling at 1–2% for 10 kA events.

[30] We next examine the distribution of NLDN-reported peak current for the 13.6 million events (both IC and CG) processed by the CMCN in the 3 year analysis window. Figure 4 shows the distributions for positive and negative polarity events. As expected, these distributions of I_{pk} of those events processed by the CMCN do contain fewer low peak current events than the reported distributions of peak current of all NLDN-measured events [*Cummins et al.*, 1998a; *Lightning and Insulator Subcommittee of the T&D Committee*, 2005].

[31] However, despite the low DE at low NLDN I_{pk}, the distributions show that the CMCN measured many lightning events across the entire range of I_{pk}, and the full distribution of lightning events that occur in the U.S. have been extensively sampled. Even for the lowest values of I_{pk} (10–20 kA), the CMCN still measured approximately 2 million events. While this is a small fraction of the total number of NLDN events in this range, it is more than sufficient to generate meaningful iCMC statistics. There is some unavoidable geographic bias in the measured low I_{pk} events, because they must be close to one of our two sensors. It is difficult to quantify this bias, but the sensor locations in Colorado and North Carolina ensure that different meteorological conditions are sampled by each.

[32] We correct this detection efficiency in our analysis of the overall iCMC distribution described in section 4.2. However, many of the results that follow are based primarily on high I_{pk} strokes (sections 4.3 and 5) or rely simply on having a large number of measured lightning events, such as the relationship between I_{pk} and iCMC (section 4.4). These results will not be significantly affected by low detection efficiency for these smaller events.

4.2. CMCN iCMC Distributions

[33] Figure 5 shows the raw distribution of CMCN-measured impulse charge moment change (iCMC) for the 13.6 million strokes processed by the CMCN in the 3 year analysis window. Positive and negative polarity events are again separated. Throughout the paper, we explicitly use a – sign to denote iCMC when discussing only negative strokes, although when comparing the iCMC for positive and negative strokes in plots or in the text, we use the unsigned iCMC magnitude. This distribution underestimates the number of low iCMC events because of the low detection efficiency of small I_{pk} events. We can compensate for this and generate estimated corrected distributions that reflects the iCMC distributions for all NLDN-detected events by the following procedure. We first compute the iCMC distribution for a narrow range of I_{pk} from the directly measured data. Next, we compute from the detection efficiency the number of additional lightning events in that narrow I_{pk} range that would have been computed with an ideal network that detected all NLDN events. We then multiply this iCMC distribution by this number of additional strokes, add that distribution to the measured iCMC distribution, and repeat over all ranges of I_{pk}. By assuming that the missing strokes follow the same iCMC distribution as the measured strokes, we can thus derive these corrected iCMC shown in dashed lines in Figure 5 that represent the best estimate we can make of the statistical distribution of iCMC in all NLDN-detected lightning.

[34] We base much of the analysis that follows on these corrected distributions. The expected longer tail in the positive polarity distribution is evident. Positive and negative strokes occur with equal absolute frequency at an iCMC of 105 C km, while at high iCMC values (from about 500 C km up to about 1000 C km, the maximum value with meaningful statistics), positives are approximately 10 times more frequent than negative strokes. This is consistent with past measurements of impulse charge transfer [*Berger et al.*, 1975] and also with reported measurements of much longer duration (not impulse) lightning charge moment changes from Schumann resonance band radio measurements [*Williams et al.*, 2007].

[35] Almost the entire corrected negative iCMC distribution and the upper end of the corrected positive distribution are well-fit with log-normal functions. Using the standard formula $f(x) = \frac{1}{x\sigma\sqrt{2\pi}} \exp(-\frac{(\ln x - \mu)^2}{2\sigma^2})$, with x denoting iCMC in C km (thus x is the dimensionless number formed by normalizing the iCMC by 1 C km), μ the location parameter and σ the scale parameter, fits were obtained and are plotted in Figure 5. For negative strokes, we find that $\mu = 1.10$ and $\sigma = 1.40$ fits the shape of the entire observed distribution from about –15 C km to almost –1000 C km and over more than six orders of magnitude in occurrence rate.

[36] The parameters $\mu = 3.40$ and $\sigma = 1.12$ fit the positive iCMC distribution for values from +70 C km to almost +2000 C km, which spans more than 5 orders of magnitude in occurrence rate. However, there is an excess of small iCMC (+5 to +70 C km) positive events that cannot be fit

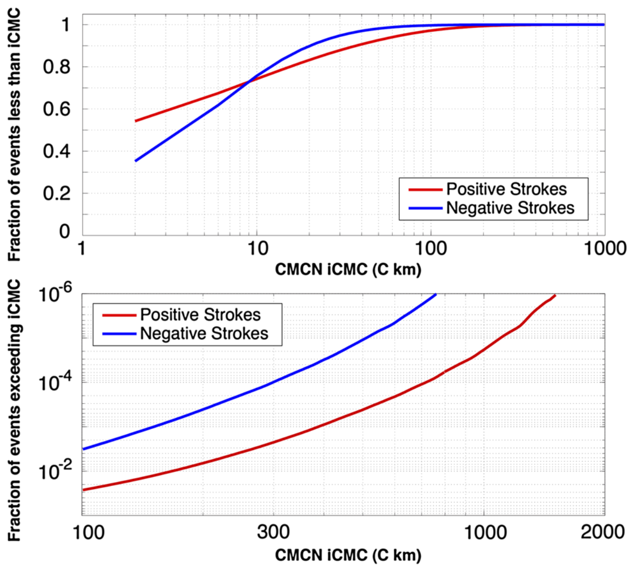

Figure 6. Cumulative distribution functions (CDFs) of iCMC for positive and negative events based on the detection-efficiency corrected distributions. (top) Traditional CDF spanning the entire range of measured iCMC values for each polarity. (bottom) Plot showing the fraction of observed lightning events that exceed a given iCMC value to highlight the relative occurrence rate of very high iCMC strokes.

with a log-normal distribution that also fits the high end of the distribution. One possibility is that the low iCMC events are dominated by +ICs, while the higher iCMC events are predominantly +CGs. These are distinct physical processes, and it is reasonable that they might exhibit different iCMC statistical distributions. This can be tested by examining the iCMC distribution for events identified by the NLDN as +IC. As shown in the figure, this distribution does exhibit significantly more small iCMC events, suggesting the possibility that these small iCMC events are +ICs.

[37] However, still about half of the observed small (below about 10 C km) iCMC positive events are classified as CG. Also, approximately 10% of the high iCMC positive events are classified as +IC by NLDN. Based on the large charge transfer, it seems possible that these are in fact +CG strokes based on their high impulse charge transfer, as previous measurements of IC flash charge transfer have not shown tens of C moving in two ms or less [*Rakov and Uman*, 2003, p. 325]. These issues highlight the challenge of distinguishing between IC and CG events and also suggests that the measured iCMC may be able to provide additional information to better distinguish IC and CG events.

[38] Figure 6 shows the same corrected positive and negative iCMC distributions as cumulative distribution functions (CDFs) to more easily visualize the relative occurrence rate of lightning events exceeding given iCMC values. Note that these are from the corrected iCMC distributions and thus represent occurrence rates relative to all NLDN-reported lightning events. The corrected distributions should thus be evaluated relative to corrected totals of 144 million negative and 27 million positive lightning events.

[39] The median (50%) iCMCs are very small, with –3.9 C km for negatives and < 2 C km for positives. These values are smaller than those in past measurements of charge transfer or charge moment change [*Brook et al.*, 1962; *Berger et al.*, 1975; *Cummer and Lyons*, 2004]. However, it should be noted that past studies analyzed up to hundreds of events, while the statistics presented here are based on millions of strokes spanning essentially all types of storms that occur within the U.S. and include both IC and CG lightning event populations. By correcting the CMCN detection efficiency as we have, these statistics include a much larger fraction of small lightning events than have been included in previous studies.

[40] For all negative polarity events, the corrected iCMC distribution gives a mean value of –10.2 C km. Strokes identified by NLDN as negative IC are only about 1% of the total negative event population, and we can thus consider this the mean negative CG iCMC of the entire population of NLDN events with I_{pk} > 10 kA. The mean of the corrected iCMC distribution for all positive events is +15.6 C km. This value combines CGs with a significant fraction of ICs, however.

[41] Figure 6(bottom) focuses on the high iCMC portion of the distributions to highlight the occurrence rate of these unusually strong lightning flashes. These are relative frequencies within each polarity. For example, negative strokes that exceed roughly –750 C km are 10^{-6} of all negative strokes in the corrected data set, and thus the distribution predicts that approximately 144 of these events (10^{-6} times the corrected negative event total of 144 million) occurred in the U.S. in 36 months. The actual number of negative events above –750 C km in magnitude was 138. Similarly, positive strokes exceeding +1400 C km occurred at the same 10^{-6} relative rate. With a corrected total of 27 million positive events, the distribution predicts about 27 of these events U.S. in the 3 year window, and precisely 27 such events were observed by the CMCN.

4.3. Implications for Sprite Occurrence Rates

[42] Lightning-driven electric breakdown in the upper atmosphere creates the class of transient luminous event known as sprites [*Pasko*, 2010]. It has been established theoretically [*Pasko et al.*, 1997] that the high altitude electric field is most closely related to the lightning charge moment change, and measurements have shown that sprite generation is driven largely by this parameter [*Hu et al.*, 2002; *Cummer and Lyons*, 2005; *Li et al.*, 2008]. Remote measurements of lightning charge moment change are one of the best tools for estimating the sprite occurrence rate over large areas and long times [e.g., *Füllekrug and Constable*, 2000]. The CMCN measurements reported here provide an opportunity to examine this issue over the entire U.S. and in a 3 year time window.

[43] For the purposes of estimation, we assume that an impulse charge moment change of +300 C km during local nighttime is required to create a prompt positive-polarity sprite [*Cummer and Lyons*, 2005], one that initiates within a few milliseconds of a +CG. We also assume that a nighttime iCMC of –500 C km is required to create a negative-polarity sprite [*Li et al.*, 2012] (all reported negative sprites have been prompt). From Figure 6, the fraction of NLDN-detected positive-polarity lightning events that exceed +300 C km is 2×10^{-3}. We find that 71% of these high iCMC positive events occurred during local nighttime. A corrected 27 million positive events in 3 years thus gives an annual

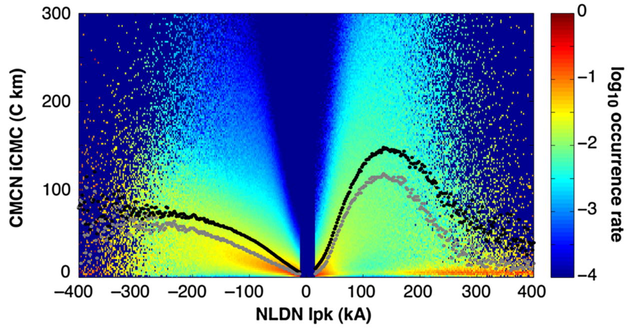

Figure 7. Normalized scatter density plot of iCMC versus I_{pk} for 13.1 million NLDN-identified CG strokes in the data set. Each vertical slice denotes the probability distribution function of iCMC (on a logarithmic color scale) for the given value of I_{pk}, and the mean and median iCMC for each value of I_{pk} are marked with black and gray dots, respectively.

rate of about 13,000 prompt positive sprites per year over the U.S. Similarly, the fraction of negative polarity NLDN lightning events that exceed –500 C km is 10^{-5}, and we find that 73% of these high iCMC negative events occurred during local nighttime. A corrected 144 million negative events in 3 years thus gives an estimated annual rate of about 350 negative polarity sprites per year over the U.S.

[44] Many positive sprites are delayed significantly from a return stroke due to long continuing currents in positive lightning [*Cummer and Füllekrug*, 2001]. Observations suggest that 30%–50% of positive sprites are prompt [*Li et al.*, 2008], and thus a bit more than half of sprites are delayed. Assuming 60% of sprites are delayed results in an estimate of the total number of positive sprites over the U.S. as roughly 35,000 per year. Satellite observations have yielded an estimated global sprite occurrence rate of 260,000 per year [*Chen et al.*, 2008]. Analysis of several months of Schumann resonance-band radio observations [*Füllekrug and Constable*, 2000; *Sato and Fukunishi*, 2003; *Ignaccolo et al.*, 2006] have yielded similar numbers (although roughly ∼4 times higher). Given that the United States is known to be one of four or five regions where sprites are common, these global estimates are in reasonable agreement with our estimate of 35,000 positive sprites per year in the U.S. This estimate is sensitive to the assumed iCMC threshold, as +200 C km iCMC strokes are five times more common than +300 C km strokes and thus could easily be shifted upwards by a factor of 2 or more.

[45] The CMCN measurements indicate that negative sprites should be roughly 100 times less frequent than positive sprites, based on the assumptions above. Recent work [*Williams et al.*, 2007] has called attention to the apparent paradox between the rarity of negative polarity sprites (taken as 1000:1 in that paper based on reported observations) given that, according global charge moment change (long duration, not impulse) measurements from SR-band observations have suggested that high charge moment change negative strokes are only about 10 times less frequent than similar positive strokes (which agrees well with our measurements in Figure 5). It should be noted that newer optical measurements indicate that the ratio of positive to negative sprites is probably closer to 200:1 [*Li et al.*, 2012]. Our geographic analysis in section 5.2 indicates that the estimated 1000:1 ratio [*Williams et al.*, 2007] may be biased by many sprite observations having occurred in Colorado and New Mexico, and these sites cannot see to the distances where high iCMC negative strokes more frequently occur in the U.S. (see Figure 13).

[46] The 100:1 ratio predicted from these measurements thus comes from two factors. One is that high iCMC positives are only 10 times more frequent than negatives for a fixed iCMC. The other comes from the experimentally observed factor-of-2 difference in the charge moment change threshold required to actually create sprite streamers of negative and positive polarity in the mesosphere [*Taylor et al.*, 2008; *Li et al.*, 2012]. Figure 6 shows that the frequency of negative strokes with iCMC above –500 C km (roughly the negative sprite threshold) is almost exactly 10 times less than that for –300 C km strokes. These two factors of 10 combine to give the 100:1 ratio. As noted by *Williams et al.* [2007, 2012], the halo, a diffuse and dimmer optical emission, has been neglected in this analysis, and we agree that there are likely many unobserved halos occurring for negative lightning in the –300 to –500 C km iCMC range.

4.4. The Relationship of Peak Current and iCMC in NLDN CG Strokes

[47] The I_{pk} and iCMC distributions in Figures 4 and 5 have similar shapes and one might reasonably ask how well correlated these two parameters are. Measurements of close to 100 rocket-triggered strokes [*Schoene et al.*, 2010] suggest that, over a 1 ms time window, they are connected but not especially well correlated. We show below that the measurements of millions of strokes reported here supports that conclusion and further defines the relationship between these quantities, which is strongly polarity-dependent. In this section we focus only on strokes identified as CG by the NLDN.

[48] Figure 7 shows a normalized scatter density plot of these two values for the 13.1 million NLDN-identified CG strokes in the data set. The strokes are first binned in the I_{pk}-iCMC plane with 2 kA and 2 C km resolution. Then, for each value of I_{pk}, the stroke count for each value of iCMC is divided by the total number of strokes (for all iCMC values) for that 2 kA range of I_{pk}. This results in a plot in which each vertical slice (fixed I_{pk}, all iCMC) is the iCMC probability distribution function for that narrow 2 kA range of v. The mean value of iCMC for each I_{pk} bin is marked with a black dot.

4.4.1. Negative CGs

[49] For NLDN-classified negative CGs, there is a clear peak in the iCMC distribution that increases with I_{pk}, indicating a statistical link between these two parameters. That said, there is considerable spread in the iCMC distribution for a given I_{pk}. Figure 8(top) shows the distributions of iCMC (normalized to a peak of unity) for three different ranges of I_{pk} wide enough to contain more than 10^4 strokes. All three of these distributions have distinct peaks but long tails in iCMC, as shown in Figure 7 where, for a given I_{pk}, the mean iCMC is close to twice the mode of the distributions. This shows that I_{pk} and iCMC are connected, but that one cannot be used to predict the other reliably in individual negative CG strokes. Section 4.4.3 describes in more detail the numerical relationship between I_{pk} and iCMC.

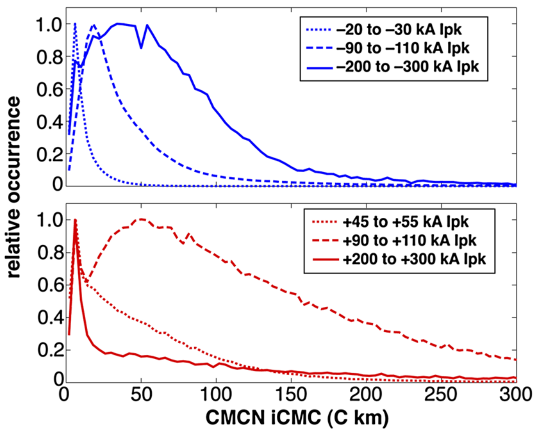

Figure 8. Normalized distributions of iCMC for three different ranges of NLDN I_{pk} that show the substantial spread in iCMC for narrow ranges of I_{pk}. (top) Negative CG strokes. (bottom) Positive CG strokes.

4.4.2. Positive CGs

[50] The connection between I_{pk} and iCMC in NLDN-classified positive CG strokes is even weaker than that for negative CGs and exhibits additional interesting features. Figure 7 shows a very broad spread of iCMC for almost all values of I_{pk}, and this is confirmed by the similarly broad normalized distributions of iCMC for three ranges of I_{pk} shown in Figure 8(bottom). Thus, in positive CG strokes, I_{pk} and iCMC are at best weakly connected, and one cannot be used to reliably predict the other.

[51] The I_{pk}-iCMC relationship for positive CGs also exhibits distinct differences with I_{pk}, unlike for negative CGs. For low peak currents (<40 kA), the distribution is dominated by small iCMC values that have almost no link to I_{pk} (see the red region close to the origin for the positive polarity strokes in Figure 7). Even for I_{pk} as high as 45 to 55 kA, the distribution in Figure 8 shows that it has a peak of low iCMC (<20 C km) strokes. As noted above in section 4.2, some of these events are possibly ICs even though NLDN identified them as CG.

[52] For positive CGs with peak current between 50 kA and roughly 200 kA, Figure 7 shows a very broad distribution of iCMC spanning a few tens to a few hundred C km. This very long tail is evident in the iCMC distribution for 90 to 110 kA positive CGs shown in Figure 8. For these +CGs, iCMC and I_{pk} are not at all well correlated, and iCMC can almost be considered an independent measurement.

[53] Most surprising is the distribution for very high I_{pk} (>200 kA). Figure 7 shows a distribution peak at very low iCMC for these, which is also clear in the iCMC distribution for 200 to 300 kA positive CGs shown in Figure 8. These low iCMC strokes are present at levels that actually make the mean iCMC drop as I_{pk} increases above about 150 kA. Thus, the high I_{pk} strokes appear to represent two distinct populations: a low iCMC (less than 20 C km) group, and a very broad tail of higher iCMC strokes that range from a few tens to many hundreds of C km.

[54] Initial examination of the raw data for these very high I_{pk}/very low iCMC NLDN-classified +CGs show that some are negative polarity events whose polarity was incorrectly identified by the NLDN. The CMCN processing relies on the NLDN-reported polarity, and anomalously small values will be computed when the polarity is wrong. But some of these are positive polarity events with very small iCMCs and are thus an interesting class of extremely high peak current and very low charge moment strokes. We suggest that they could be IC events misidentified by the NLDN, but more analysis is needed to determine what they are.

4.4.3. Fits to the Mean iCMC

[55] Figure 9 shows the mean iCMC and the mean plus one standard deviation of iCMC as a function of I_{pk} for CG-identified NLDN strokes. The standard deviation is almost equal to the mean for both negative and positive polarity strokes, further confirming the long-tailed iCMC distributions for a given I_{pk} and that the connection between these parameters varies significantly from stroke to stroke.

[56] But even though the correlation between iCMC and I_{pk} is broad, it may be useful to have simple analytical forms that enable computation of the mean iCMC for a given I_{pk}. For negative CGs with I_{pk} from –10 to –200 kA, we find that a good analytical fit to the mean iCMC (denoted with the bar notation) is obtained with

$$\overline{\mathrm{iCMC}}^{-}(\mathrm{C\ km}) = 0.53|I_{pk}(\mathrm{kA})| - 0.00086 I_{pk}^2(\mathrm{kA}). \quad (1)$$

This means that 0.53 is the linear scaling factor from I_{pk} in kA to mean iCMC in C km for negative CG strokes with peak current magnitude less than about 120 kA. At higher peak currents, the slope of the iCMC begins to drop, which is reflected in the quadratic term in the analytical fit. This could reflect an actual drop in the scaling from I_{pk} to iCMC for high peak current strokes, but we think it may originate from challenges in correctly classifying the polarity or type of high peak current strokes.

[57] The shape of the mean iCMC for positive CGs is more complex. For positive CGs with I_{pk} from +40 to +200 kA, a good analytical fit to the mean iCMC is

$$\overline{\mathrm{iCMC}}_{hi}^{+}(\mathrm{C\ km}) = -59.36 + 2.78|I_{pk}(\mathrm{kA})| - 0.0092 I_{pk}^2(\mathrm{kA}). \quad (2)$$

Thus positive CGs exhibit a much larger I_{pk}-to-iCMC linear scaling factor of 2.78 (with a y-intercept of –59), reflecting a

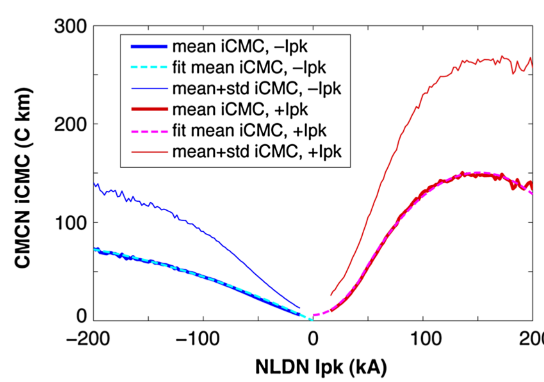

Figure 9. Computed iCMC mean and standard deviation as a function of NLDN I_{pk}. The high standard deviation confirms the long tailed-nature of the iCMC-I_{pk} statistical distributions. Also shown are the analytical fits to the mean iCMC for positive and negative strokes.

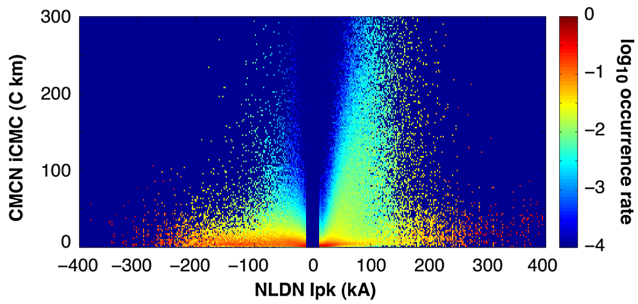

Figure 10. Normalized scatter density plot of iCMC versus I_{pk} for 460,000 NLDN-identified IC events in the data set. Each vertical line denotes the probability distribution function of iCMC (on a logarithmic color scale) for the given value of I_{pk}.

significantly higher impulse charge moment for a given peak current. Again, a quadratic term is needed to capture deviations at higher peak currents (above about +100 kA) that for NLDN-identified positive CGs cause the mean iCMC to shrink as I_{pk} increases. As discussed above, however, this may be due to a population of unusually high peak current +IC strokes that are misidentified as +CGs.

[58] For strokes below +40 kA, a different functional form is needed which is not surprising as these strokes are also probably dominated by misidentified +ICs. From +10 to +40 kA, a good analytical fit to the mean iCMC is

$$\overline{\mathrm{iCMC}}^{+}_{lo}\,(\mathrm{C\ km}) = 5.90 + 0.020 I_{pk}^{2}, (\mathrm{kA}). \quad (3)$$

4.5. The Relationship of Peak Current and iCMC in NLDN IC Strokes

[59] The relationship between I_{pk} and iCMC for the events classified as IC by the NLDN is, not surprisingly, different from that for CGs. Figure 10 shows the normalized scatter density plot for these 460,000 IC events in our database. Negative ICs exhibit an essentially flat and low (<20 C km) distribution of iCMC for all values of I_{pk}. The presence of negative polarity IC-classified events with peak currents above 100 kA in magnitude is surprising, although whether some fraction of these results from NLDN polarity errors needs to be investigated.

[60] For positive ICs, we again see a fairly flat iCMC distribution independent of I_{pk} that is different from those events reported as CG. A small but detectable number of high iCMC events are in this distribution, and it is possible that these are actually the small fraction of +CG strokes that are misidentified as +IC. Interestingly, there are far fewer >200 kA positive events identified as IC than CG (see Figure 5), despite the fact that the small iCMC of most of these strokes suggests that they could be IC. This is further evidence that these uncommon strokes have unusual radiated waveform characteristics that may make their stroke type difficult to classify.

5. Geographic Distributions of High I_{pk} and iCMC Lightning Events

[61] We now present and explore the geographic distribution of high iCMC events of positive and negative polarity. First, Figure 11 shows a geographic scatter density plot of all 13.6 million events measured by the CMCN system. As noted previously, because of the amplitude-based trigger threshold in our sensor operation, there is a bias in which more strokes are detected close to the two sensors in North Carolina and Colorado. Any analysis of the locations of small or modest peak current strokes would thus also be geographically biased. High peak current strokes, however, trigger our system regardless of where they occur in the U.S. Consequently, the question we address here is, where do high I_{pk} and high iCMC events preferentially occur?

5.1. High I_{pk} and iCMC Positives

[62] We first focus on positive polarity events. Events classified as +CG and +IC are both included in the analysis that follows, but we assume that these high I_{pk} and iCMC events are dominated by +CG strokes. Figure 12(top) shows the smoothed geographic distribution of all positive polarity CMCN-measured events with I_{pk} > +100 kA. The geographic bias evident in Figure 11 has disappeared, indicating that these high peak current events produce large enough VLF sferics to trigger the CMCN systems regardless of range, which is consistent with the > 70% detection efficiency of the CMCN for these strokes (Figure 4). These high I_{pk} positive events are concentrated in the upper midwestern U.S. [*Lyons et al.*, 1998] with a secondary peak in the Gulf Stream off the east coast and another near the Gulf of California that is not well resolved because of the geographic limits of the NLDN data received for the CMCN.

[63] The high I_{pk} positive distribution shows a hole near our sensors in North Carolina and a steep drop in occurrence rate as one moves west from Kansas towards our sensors in Colorado. These features are seen in more comprehensive analyses of NLDN data *Orville et al.* [2011] and are thus not an artifact of the sensor proximity, but instead probably reflect that both sensors are placed just to the east of relatively large mountain ranges and are thus in rain and lightning shadow zones.

[64] Figure 12(second) shows the smoothed distribution of all CMCN events with iCMC > +100 C km. We consider these "possible" sprite-producers in the sense that the impulse CMC is not generally large enough to create a

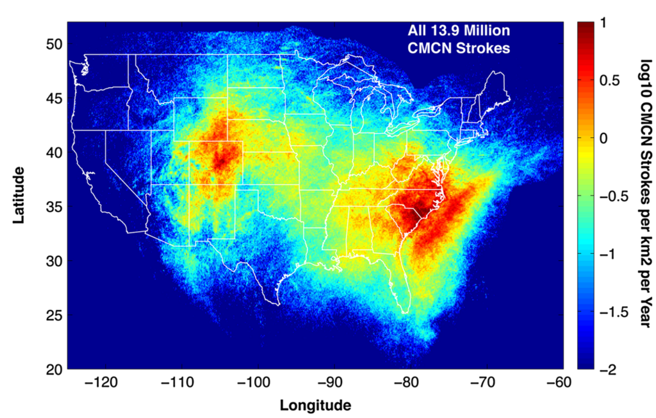

Figure 11. Geographic scatter density plot of all 13.6 million lightning events measured by the CMCN during the 3 year analysis period. The higher concentration of events near the two CMCN sensors in North Carolina and Colorado is an artifact of the amplitude triggering of the system.

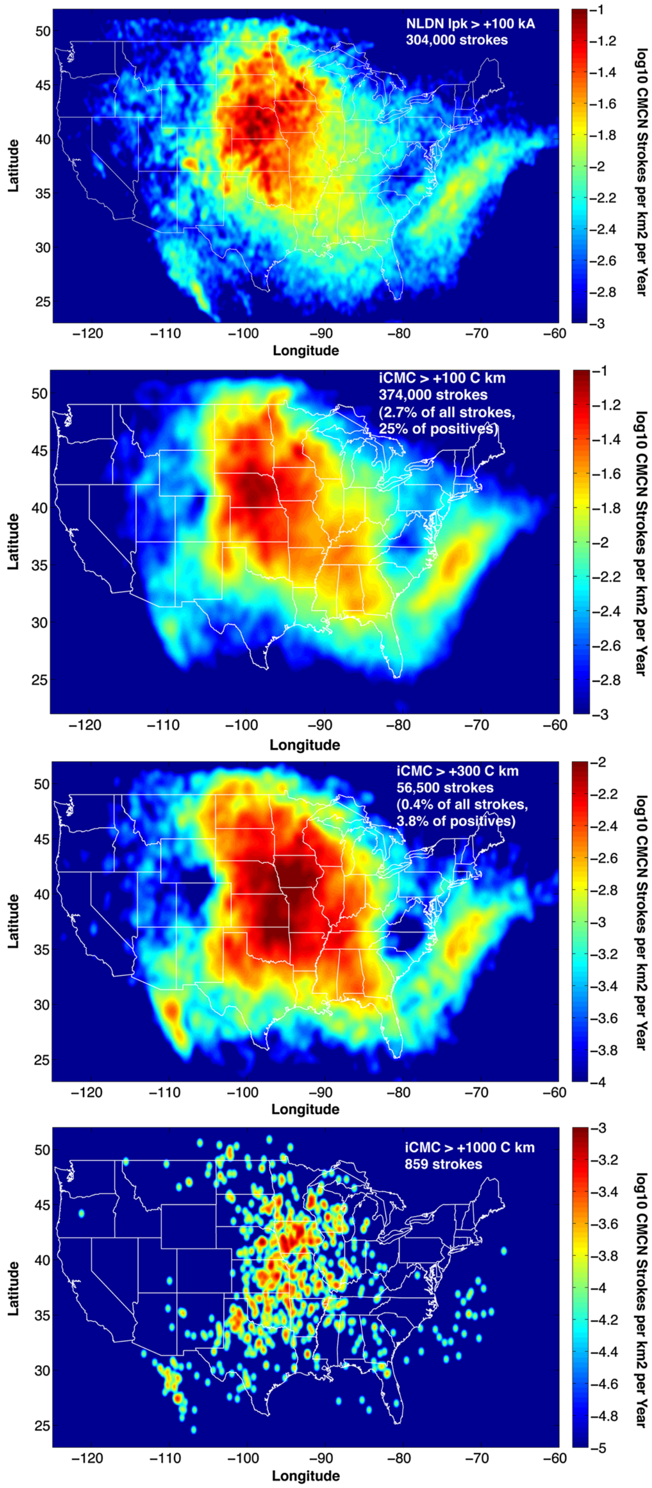

Figure 12. Geographic distributions and rates of energetic positive polarity events. (top) The distribution of events with NLDN I_{pk} > +100 kA. (second) The distribution of events with iCMC > +100 C km. (third) The distribution of events with iCMC > +300 C km. (bottom) The distribution of events with iCMC > +1000 C km.

prompt sprite, but these strokes are sometimes followed by strong continuing currents that do eventually produce a sprite. Interestingly, the I_{pk} > +100 kA and iCMC > +100 C km distributions are almost the same, with a broad peak in the midwest centered in Nebraska that extends southeast to Georgia. Note that the detection efficiency issue discussed in section 4.1 means that high iCMC events with modest peak currents are less likely to be detected by the CMCN, and the iCMC distributions are thus modestly biased against such strokes at longer distances from the sensors. The secondary peak over the Gulf Stream is, if anything, slightly stronger in this iCMC distribution, which agrees with sprites being observed relatively frequently in this area [*Li et al.*, 2012].

[65] Figure 12(third) shows the smoothed distribution for events with iCMC > +300 C km. We consider these “likely” sprite producers because the impulse CMC by itself reaches the empirical threshold for generating a sprite. The geographic peak of this distribution is noticeably shifted to the east and south from the +100 C km peak, with maximum occurrence rates of about 0.01 strokes per km^2 per year from Iowa to northeast Oklahoma. This shift reflects the eastward motion of large midwestern storms and the additional time it takes for the storms to evolve into a stage where they are capable of generating such high charge transfer lightning. But these very high iCMC events do occur regularly over a very wide portion of the United States, including the southeast (Mississippi, Alabama, etc.) where few efforts to observe sprites have been made. In Figure 12(third), the expanding holes near the Duke and Colorado sensors show that the CMCN exhibits some degree of blindness to high iCMC events at close ranges. These events trigger the system, but the signal is saturated which results in a measured iCMC that is much smaller than it actually is.

[66] Figure 12(bottom) shows the distribution for events with iCMC > +1000 C km. No reasonable degree of smoothing can generate a smooth distribution because there are only 859 events of this iCMC magnitude in the data set, but it is still interesting to see where they occur. These very high iCMC events are again concentrated in the upper midwest and centered in Iowa, with a few seen throughout the south and also a small concentration near the Gulf of California. They sometimes occur over the Gulf Stream, but they rarely occur over water, and they are almost completely absent from the Gulf of Mexico. They are also almost completely absent in the northeastern portion of the U.S.

5.2. High I_{pk} and iCMC Negatives

[67] We now focus on negative polarity events. Figure 13(top) shows the smoothed geographic distribution of all negative polarity CMCN-measured events with I_{pk} < –100 kA. These high I_{pk} negative events are concentrated most strongly in a swath of the Gulf Stream that is distinctly separated from the coast, and also occur frequently along the coast in the Gulf of Mexico. There is a modest secondary peak over land near Oklahoma and Arkansas, and an even weaker peak near the Gulf of California near the geographic limits of the NLDN data received for the CMCN. The frequency of these events drops as one moves north, and the overall high I_{pk} negative distribution is shifted significantly southward of the distribution of high I_{pk} positive events. As for the high I_{pk} positives, the high I_{pk} negative distribution shows holes near

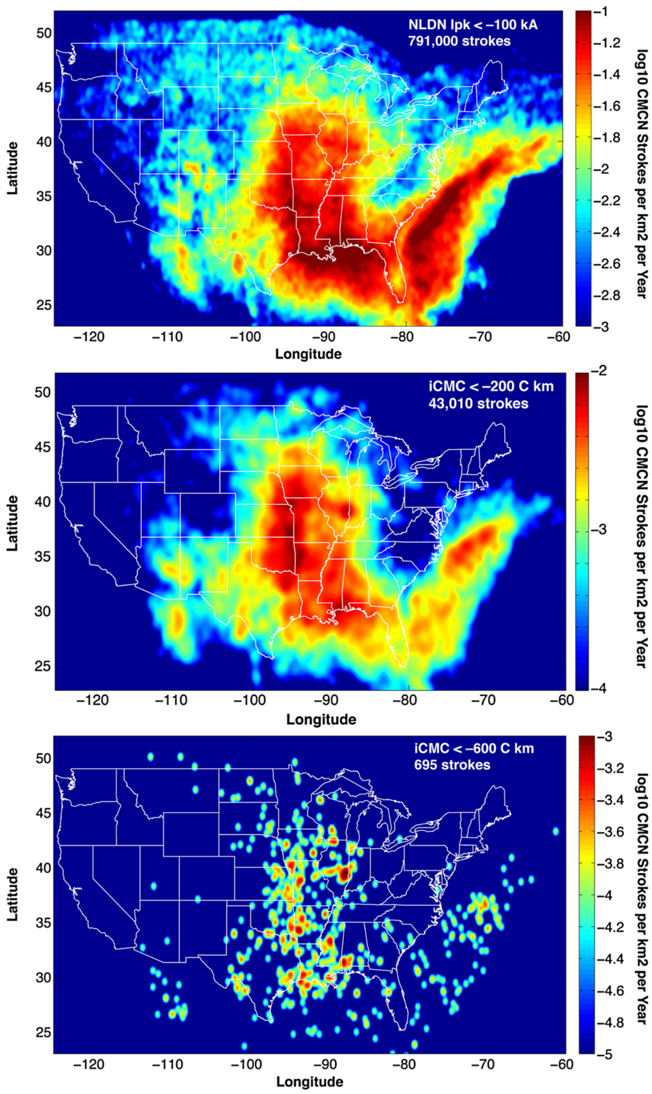

Figure 13. Geographic distributions and rates of energetic negative polarity events. (top) The distribution of events with NLDN I_{pk} < –100 kA. (middle) The distribution of events with iCMC < –200 C km. (bottom) The distribution of events with iCMC < –600 C km.

our sensors in North Carolina and Colorado that are not artifacts but reflect known inhomogeneities in the geographic distribution of lightning.

[68] Figure 13(middle) shows the smoothed distribution of all CMCN events with iCMC < –200 C km. These high charge transfer negative events are not strong enough to create sprites. Interestingly, there are distinct differences between the I_{pk} < –100 kA and iCMC < –200 C km distributions. The concentrations of strong lightning in the Gulf Stream and Gulf of Mexico remain, but they are not the highest concentrations that they were for in the high I_{pk} map. Instead, the region of high iCMC negative lightning along a nearly vertical strip from western Missouri to western Arkansas (around –95°E longitude) becomes dominant. This indicates that while high I_{pk} negative events are most frequent in the coastal Gulf of Mexico and the off-shore Gulf Stream, these are not the regions of highest iCMC negative events. Instead the highest iCMC negative events occur more frequently over land.

[69] Figure 13(bottom) shows the weakly-smoothed distribution of the 695 negative events with iCMC < –600 C km. These strokes should be considered possible negative polarity sprite-producing events, as an iCMC this high approaches the empirical threshold for driving negative streamers in the mesosphere [*Taylor et al.*, 2008; *Li et al.*, 2012]. The majority of these events occurred along a thin vertical strip between –93° and –95°E longitude from the upper midwest to the gulf coast of Texas. Some also occurred east of this strip, to approximately –87°E, but almost none occurred west of this strip. This suggests one possible reason why negative polarity sprites are seen so infrequently from the common optical observing locations in Colorado and New Mexico: the high iCMC negative polarity lightning usually occurs just a little bit too far east to be in range from these locations.

[70] The situation is equally interesting with the coastal locations. Only the very northern portion of the Gulf Stream high I_{pk} region has a significant concentration of very high iCMC negative events. Despite being a prolific producer of high I_{pk} negative events, most of the Gulf Stream does not seem to produce very high iCMC negative events. Similarly, while the entire Gulf of Mexico is an equally prolific producer of high I_{pk} negative events, only the western portion has a significant concentration of very high iCMC negative events. That only some places where high I_{pk} negative events are common seem able to produce many very high iCMC negative events probably reflects differences in the storm or meteorological conditions in these locations which are not well understood.

[71] It is also worth reiterating that most of the locations of very high iCMC negative events are not within the range of most places where high altitude optical observations have been made. The Gulf Stream peak is too far north and east to be visible with cameras at Duke University, and the midwestern locations seem just a little bit too far east for Colorado and New Mexico cameras. A few well placed cameras might be able to significantly increase the number of documented negative polarity sprites.

6. Summary and Conclusions

[72] We have analyzed 3 years of measurements of lightning impulse charge moment change (iCMC, defined as the lightning discharge charge moment change during the first 2 ms after the discharge onset) for 13.6 million NLDN-detected events over the continental United States. These measurements of iCMC are generated from a real-time lightning charge moment change network that relies on NLDN lightning geolocations provided by Vaisala, Inc. and has been operating since 2007. This network consists of two sensor stations, one in Colorado and one in North Carolina that together can measure lightning over the entire U.S. because of the long range over VLF and ELF electromagnetic signals that can be detected. There is some spatial bias in the measured events because higher peak currents are required to trigger the system for events farther from the closest sensor. However, the distribution of NLDN peak current of all measured events spans the full range of peak current, and thus all values of I_{pk} are represented in the iCMC measurements.

[73] After correction for the I_{pk}-dependent detection efficiency of the CMCN, we find that the overall statistical iCMC distribution shows that positive and negative polarity events are equally common at 105 C km, with negatives dominating below that value and positives dominating above. At 300 C km and above, positive events are about 10 times more frequent than equally large negative events. Within the population of lightning events of each polarity, the one-in-a-million iCMC levels are –750 C km and +1400 C km and thus occur only a few tens of times per year across the entire U.S.

[74] The measurements of I_{pk} and iCMC in NLDN-identified CG lightning exhibit a varying degree of correlation in individual strokes. For negative CG strokes, the mean iCMC for a given I_{pk} increases monotonically, with an iCMC standard deviation approximately equal to the mean, implying a broad distribution of iCMC for a given I_{pk}. For positive CG strokes, the iCMC distributions for fixed I_{pk} are even broader. This implies that I_{pk} can be used to predict iCMC in a statistical sense, but I_{pk} cannot predict iCMC very accurately in an individual CG stroke. These parameters should thus be considered independent measurements of the characteristics of a CG lightning stroke.

[75] For positive NLDN-identified CG strokes, the relationship between I_{pk} and iCMC exhibits a clear change above and below 20 C km. For all values of I_{pk}, there is a sharp peak with small (< 20 C km) iCMC superimposed on a much broader distribution. Remarkably, this dual distribution is even present for very high values of I_{pk} (> 200 kA). It is possible, although far from certain, that these overlapping distributions represent true CG strokes (high iCMC) and misclassified IC pulses (low iCMC). If so, then independent measurements of iCMC may help in the very challenging problem of classifying CG and IC events.

[76] Adopting iCMC thresholds for the generation of prompt sprites of +300 and –500 C km for positive and negative polarity, we estimate annual rates of 13,000 positive and 350 negative polarity prompt sprites per year over the U.S. Acknowledging that a substantial fraction of positive sprites are significantly delayed from a lightning return stroke and thus not produced by the impulse charge moment change, we estimate that the overall ratio of positive polarity to negative polarity sprites over the U.S. is approximately 100 to 1.

[77] We also examined the geographic distributions of high iCMC lightning strokes. High iCMC (> +100 C km) positive strokes occur over a broad area of the central U.S. with a peak concentration of 0.1 per km^2 per year. There is also a distinct secondary geographic peak over the gulf stream current off the east coast of the U.S. Very high iCMC (> +300 C km) positive strokes have a similar distribution but with a peak location that is clearly shifted to the east. These and ultra-high iCMC (> +1000 C km) positive strokes occur most frequently in Iowa, but do occur throughout the midwest and south.

[78] Energetic negative strokes exhibit interesting variations in distribution. High peak current (< –100 kA) negative strokes are most frequent over the gulf stream ocean and near the coastal areas of the Gulf of Mexico. In contrast, very high iCMC (< –200 C km) negative strokes are most frequent in the midwest, over land. Ultra high iCMC (< –600 C km) negative strokes are uncommon, but are most concentrated along a vertical strip in the central U.S. Interestingly, this strip is likely a bit beyond viewing from Colorado and New Mexico where most TLE viewing occurs, suggesting that the infrequent observation of negative sprites and halos in the U.S. may be partly driven by observation location. Why the locations of highest positive and negative iCMC events are not quite the same is a question that merits further investigation.

[79] The real-time nature of the CMCN measurements will continue to be valuable in nowcasting the storms and locations within storms that are generating potentially sprite-producing lightning. Additionally, these measurements will enable addressing questions related to the link between meteorology and storm structure and high charge transfer lightning. Of particular interest will be identifying the characteristics of smaller storms that are occasionally able to produce high iCMC lightning.

[80] **Acknowledgments.** We gratefully acknowledge the support of Vaisala, Inc. in providing the National Lightning Detection Network data on which the CMCN is built. Valuable feedback was provided by Ken Cummins and Amitabh Nag. We also acknowledge support from the Missile Defense Agency SBIR Program through contract HQ0006-06-C-7313, the National Science Foundation Dynamic and Physical Meteorology program through grants ATM-0642757 and ATM-1047588, and the DARPA Nimbus program through grant HR0011-10-1-0059.

References

Berger, K., R. B. Anderson, and H. Kroninger (1975), Parameters of lightning flashes, *Electra*, *80*, 223–237.

Brook, M., N. Kitagawa, and E. J. Workman (1962), Quantitative study of strokes and continuing currents in lightning discharges to ground, *J. Geophys. Res.*, *67*(2), 649–659.

Burke, C. P., and D. L. Jones (1996), On the polarity and continuing currents in unusually large lightning flashes deduced from ELF events, *J. Atmos. Terr. Phys.*, *58*(5), 531–540.

Chen, A. B., et al. (2008), Global distributions and occurrence rates of transient luminous events, *J. Geophys. Res.*, *113*, A08306, doi:10.1029/2008JA013101.

Cummer, S. A., and M. Füllekrug (2001), Unusually intense continuing current in lightning causes delayed mesospheric breakdown, *Geophys. Res. Lett.*, *28*, 495–498.

Cummer, S. A., and U. S. Inan (1997), Measurement of charge transfer in sprite-producing lightning using ELF radio atmospherics, *Geophys. Res. Lett.*, *24*(14), 1731–1734.

Cummer, S. A., and U. S. Inan (2000), Modeling ELF radio atmospheric propagation and extracting lightning currents from ELF observations, *Radio Sci.*, *35*, 385–394.

Cummer, S. A., and W. A. Lyons (2004), Lightning charge moment changes in U.S. High Plains thunderstorms, *Geophys. Res. Lett.*, *31*, L05114, doi:10.1029/2003GL019043.

Cummer, S. A., and W. A. Lyons (2005), Implications of lightning charge moment changes for sprite initiation, *J. Geophys. Res.*, *110*, A04304, doi:10.1029/2004JA010812.

Cummins, K. L., and M. J. Murphy (2009), An overview of lightning locating systems: History, techniques, and data uses, with an in-depth look at the U.S. NLDN, *IEEE Trans. EMC*, *51*, 499–518, doi:10.1109/TEMC.2009.2023450.

Cummins, K. L., M. J. Murphy, E. A. Bardo, W. L. Hiscox, R. B. Pyle, and A. E. Pifer (1998a), A combined TOA/MDF technology upgrade of the US National Lightning Detection Network, *J. Geophys. Res.*, *103*(D8), 9035–9044.

Cummins, K. L., E. P. Krider, and M. D. Malone (1998b), The US National Lightning Detection Network and applications of cloud-to-ground lightning data by electric power utilities, *IEEE Trans. Electromagn. Compat.*, *40*(4), 465–480.

Füllekrug, M., and S. Constable (2000), Global triangulation of intense lightning discharges, *Geophys. Res. Lett.*, *27*(3), 333–336.

Fuquay, D. M., A. R. Taylor, R. G. Hawe, and J. C. W. Schmid (1972), Lightning discharges that caused forest fires, *J. Geophys. Res.*, *77*(12), 2156–2158.

Hobara, Y., N. Iwasaki, T. Hayashida, M. Hayakawa, K. Ohta, and H. Fukunishi (2001), Interrelation between ELF transients and ionospheric disturbances in association with sprites and elves, *Geophys. Res. Lett.*, *28*, 935–938.

Hu, W., S. A. Cummer, W. A. Lyons, and T. E. Nelson (2002), Lightning charge moment changes for the initiation of sprites, *Geophys. Res. Lett.*, *29*(8), 120-1–120-4, doi:10.1029/2001GL014593.

Huang, E., E. Williams, R. Boldi, S. Heckman, W. Lyons, M. Taylor, T. Nelson, and C. Wong (1999), Criteria for sprites and elves based on Schumann resonance observations, *J. Geophys. Res.*, *104*(D14), 16,943–16,964.

Ignaccolo, M., T. Farges, A. Mika, T. H. Allin, O. Chanrion, E. Blanc, T. Neubert, A. C. Fraser-Smith, and M. Füllekrug (2006), The planetary rate of sprite events, *Geophys. Res. Lett.*, *33*, L11,808, doi:10.1029/2005GL025502.

Inan, U., and A. Inan (2000), *Electromagnetic Waves*, Prentice-Hall, Upper Saddle River, NJ.

Jones, D. L., and D. T. Kemp (1971), The nature and average magnitude of the sources of transient excitation of Schumann resonances, *J. Atmos. Terr. Phys.*, *33*, 557.

Lang, T., W. A. Lyons, S. A. Rutledge, J. D. Meyer, D. R. MacGorman, and S. A. Cummer (2010), Transient luminous events above two mesoscale convective systems: Storm structure and evolution, *J. Geophys. Res.*, *115*, A00E22, doi:10.1029/2009JA014500.

Latham, D. J., and J. A. Schlieter (1989), Ignition probabilities of wildland fuels based on simulated lightning discharges, *Tech. Rep. INT-411*, U.S. Dept. Agriculture.

Li, J., and S. Cummer (2012), Relationship between sprite streamer behavior and lightning-driven electric fields, *J. Geophys. Res.*, *117*, A01317, doi:10.1029/2011JA016843.

Li, J., S. A. Cummer, W. A. Lyons, and T. E. Nelson (2008), Coordinated analysis of delayed sprites with high speed images and remote electromagnetic fields, *J. Geophys. Res.*, *113*, D20206, doi:10.1029/2008JD010008.

Li, J., S. A. Cummer, G. Lu, and L. Zigoneanu (2012), Charge moment change and lightning-driven electric fields associated with negative sprites and halos, *J. Geophys. Res.*, *117*, A09310, doi:10.1029/2012JA017731.

Lightning and Insulator Subcommittee of the T&D Committee (2005), Parameters of lightning strokes: A review, *IEEE Trans. Power Delivery*, *20*, 346–358, doi:10.1109/TPWRD.2004.835039.

Lu, G., S. A. Cummer, J. Li, F. Han, D. M. Smith, and B. W. Grefenstette (2011), Characteristics of broadband lightning emissions associated with terrestrial gamma ray flashes, *J. Geophys. Res.*, *116*, A03,316, doi:10.1029/2010JA016141.

Lu, G., S. A. Cummer, R. J. Blakeslee, S. Weiss, and W. H. Beasley (2012), Lightning morphology and impulse charge moment change of high peak current negative strokes, *J. Geophys. Res. Atmos.*, *117*, D04212, doi:10.1029/2011JD016890.

Lyons, W. A., M. Uliasz, and T. E. Nelson (1998), Climatology of large peak current cloud-to-ground lightning flashes in the contiguous United States, *Mon. Weather Rev.*, *126*, 2217–2233.

Lyons, W. A., M. A. Stanley, J. Meyer, T. Nelson, S. Rutledge, T. Lang, and S. Cummer (2009), The meteorological and electrical structure of TLE-producing convective storms, in *Lightning: Principles, Instruments and Applications*, edited by H. D. Betz, pp. 389–417, Springer Science+Business Media B.V.

Orville, R. E., G. R. Huffines, W. R. Burrows, and K. L. Cummins (2011), The North American Lightning Detection Network (NALDN)—Analysis of flash data: 2001–09, *Mon. Weather Rev.*, *139*, 1305–1322, doi:10.1175/2010MWR3452.1.

Pasko, V. P. (2010), Recent advances in theory of transient luminous events, *J. Geophys. Res.*, *115*, A00E35, doi:10.1029/2009JA014860.

Pasko, V. P., U. S. Inan, T. F. Bell, and Y. N. Taranenko (1997), Sprites produced by quasi-electrostatic heating and ionization in the lower ionosphere, *J. Geophys. Res.*, *102*(A3), 4529–4561.

Rakov, V. A., and M. A. Uman (2003), *Lightning*, Cambridge University Press, Cambridge.

Ross, M., S. A. Cummer, T. K. Nielsen, and Y. Zhang (2008), Simultaneous remote electric and magnetic field measurements of lightning continuing currents, *J. Geophys. Res.*, *113*, 20,125, doi:10.1029/2008JD010294.

Sato, M., and H. Fukunishi (2003), Global sprite occurrence locations and rates derived from triangulation of transient Schumann resonance events, *Geophys. Res. Lett.*, *30*(16), 1859, doi:10.1029/2003GL017291.

Schoene, J., M. A. Uman, and V. A. Rakov (2010), Return stroke peak current versus charge transfer in rocket-triggered lightning, *J. Geophys. Res. Atmos.*, *115*, D12107, doi:10.1029/2009JD013066.

Taranenko, Y. N., U. S. Inan, and T. F. Bell (1993), Interaction with the lower ionosphere of electromagnetic pulses from lightning—Heating, attachment, and ionization, *Geophys. Res. Lett.*, *20*(15), 1539–1542.

Taylor, M. J., et al. (2008), Rare measurements of a sprite with halo event driven by a negative lightning discharge over Argentina, *Geophys. Res. Lett.*, *35*, L14812, doi:10.1029/2008GL033984.

Wait, J. R. (1970), *Electromagnetic Waves in Stratified Media*, Pergamon, Oxford.

Willett, J. C., V. P. Idone, R. E. Orville, C. Leteinturier, A. Eybert-Berard, L. Barret, and E. P. Krider (1988), An experimental test of the transmission-line model of electromagnetic radiation from triggered lightning return strokes, *J. Geophys. Res.*, *93*(D4), 3867–3878.

Williams, D. P., and M. Brook (1963), Magnetic measurements of thunderstorm currents, *J. Geophys. Res.*, *68*(10), 3243–3247.

Williams, E., E. Downes, R. Boldi, W. Lyons, and S. Heckman (2007), Polarity asymmetry of sprite-producing lightning: A paradox?, *Radio Sci.*, *42*, RS2S17, doi:10.1029/2006RS003488.

Williams, E., et al. (2012), Resolution of the sprite polarity paradox: The role of halos, *Radio Sci.*, *47*, RS2002, doi:10.1029/2011RS004794.

Yamashita, K., Y. Otsuyama, Y. Hobara, M. Sekiguchi, Y. Matsudo, M. Hayakawa, and V. Korepanov (2009), Global distribution and characteristics of intense lightning discharges as deduced from ELF transients observed at Moshiri (Japan) , *J. Atmos. Electr.*, *29*, 71–80.